

2006-01-01

Geographic Variation of Solar Water Heater Performance in Europe

Y. Yohanis
University of Ulster

O. Popel
Academy of Sciences Russia

S. Frid

See next page for additional authors

Follow this and additional works at: <https://arrow.tudublin.ie/dubenart>



Part of the [Mechanical Engineering Commons](#)

Recommended Citation

Yohanis, Y., Popel, O., Frid, S. & Norton, B. (2006). Geographic Variation of Solar Water Heater Performance in Europe. *Proceedings of the Institution of Mechanical Engineers, Part A, Journal of Power and Energy* vol.220, pp.395-407. doi:10.1243/095765006X76018

This Article is brought to you for free and open access by the Dublin Energy Lab at ARROW@TU Dublin. It has been accepted for inclusion in Articles by an authorized administrator of ARROW@TU Dublin. For more information, please contact arrow.admin@tudublin.ie, aisling.coyne@tudublin.ie, vera.kilshaw@tudublin.ie.

Authors

Y. Yohanis, O. Popel, S. Frid, and Brian Norton

Geographic variation of solar water heater performance in Europe

Y G Yohanis^{1*}, O Popel², S E Frid², and B Norton³

¹Thermal Systems Engineering Group, Faculty of Engineering, University of Ulster, Northern Ireland, UK

²Institute for High Temperatures (IVTAN), Russian Academy of Sciences, Moscow, Russia

³Dublin Institute of Technology, Dublin, Ireland

The manuscript was received on 5 March 2005 and was accepted after revision for publication on 11 October 2005.

DOI: 10.1243/095765006X76018

Abstract: Solar water heater (SWH) performance has been analysed using the ‘number of days’ method for 147 different sites in all European countries. The total number of days that the temperature of delivered solar heated water reaches or exceeds specified demand temperatures is correlated with solar radiation on a horizontal surface for summer, warm half-year, and whole year periods. Maps are presented and discussed showing the contours for the number of days that an illustrative SWH met different hot water demand temperatures. Correlations between number of days water is provided at a specified temperature and solar fractions for the same periods are determined.

Keywords: solar water heating, solar water heaters, geographic variations

1 INTRODUCTION

Although an established technology, solar water heating is still undergoing significant research and development [1]. This has been devoted increasingly to the reduction of initial installed capital cost. In the European Union, there is a substantial and growing solar water heating market [2], though its uneven development as can be seen from Table 1 reflects the relative effectiveness of market stimulation interventions. These may be aided by long-term performance characterization techniques understandable readily by consumers.

Solar water heater (SWH) design and long-term performance characterization methods have been categorized as [3, 4]: (a) utilizability based; (b) empirical correlations; (c) simplified analysis; and (d) 1-day repetitive simulations. Common to all such techniques is determination of a solar savings fraction. Yohanis *et al.* [5] proposed a method for SWH long-term performance characterization in which the number of days in each month (or in any given period of a year) when the temperature

of solar heated water in SWH storage tank reaches or exceeds a specified demand temperatures is calculated. In addition to the ‘solar savings fraction’ [6], this ‘number of days’ method provides easily understood alternative SWH performance information for a potential SWH user’s particular location, thus simplifying consumer decision-making. In this paper, the ‘number of days’ method is applied for performance analysis of solar water heating systems across Europe and empirical correlations and geographic variations derived.

2 SOLAR WATER HEATING SYSTEM SPECIFICATION

A pumped circulation SWH consisting of a flat-plate solar collector, a thermally insulated hot water storage tank and connecting pipes is considered as shown in Fig. 1. The circulation pump is actuated by a differential temperature controller, which interrupts water circulation in the system when the water temperature at the outlet from the collector falls below a specified value. Appropriate dead bands for temperature differences between inlet and outlet of solar collector are assumed to prevent unnecessary switching on and off of the pump. Water mass

*Corresponding author: Thermal Systems Engineering Group, Faculty of Engineering, University of Ulster, BT37 0QB Northern Ireland, UK.

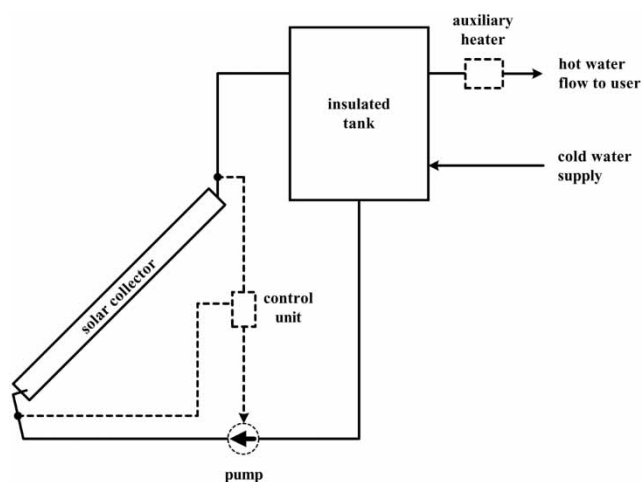
Table 1 Installed solar water collector areas in Europe

Country	Installed collector area per 1000 population (m ²)
Austria	288.89
Greece	283.43
Denmark	60.63
Germany	45.13
Switzerland	36.11
Portugal	25.00
Sweden	25.00
Netherlands	13.48
Spain	11.42
France	9.90
Finland	5.87
Italy	5.45
United Kingdom	3.49
Belgium	2.35
Ireland	0.87

flowrate in the loop is assumed to be large enough (50 kgm⁻²h⁻¹ or higher) to provide a solar collector flow factor (F'') approaching 1. The dependence of the solar collector heat removal factor, F_R , on flowrate at this or a higher flowrate is thus negligible [7].

The following points are assumed.

1. An auxiliary heater is installed in series rather than within the storage tank to provide supplementary heating if the temperature of water withdrawn from the storage tank is below that required.
2. Each day's consumption of hot water follows the same pattern and takes place in the evenings (for the base case, total daily hot water consumption is assumed to be equal to the storage tank volume). Daily distributed water consumption compared with only nighttime consumption results in higher solar fractions due to higher solar collector efficiencies arising from lower

**Fig. 1** A pumped circulation solar water heating system

3. The storage tank and all connecting pipes are well insulated thermally.
4. Because the storage tank and connecting pipes are assumed to be well insulated, simultaneous proportional changing of total solar heated water consumption volume V_{day} , store volume V_{st} , and collector area A_{sc} SWH system operation are assumed to give equivalent thermal performance.
5. The water in the storage tank is well mixed thermally, that is, there is no temperature stratification of the water inside the tank. A stratified tank, as would be likely to ensue in reality, would provide a higher draw-off temperature. Assuming a well mixed tank thus determines a lower bound to actual performance.
6. The solar collector is assumed to be single glazed, non-selective, and installed facing due south at an inclination to the horizon equal to each local latitude. The system parameters used are given in Table 2.

The solar collector area was varied in the range of 1–4 m². Demand temperatures of 37, 45, and 55 °C are considered. TRNSYS [8] was used to generate the hourly meteorological data in the form of typical meteorological years (TMY) for each site considered using the online 'RETScreen' database [9] to provide average monthly climatic data for each site. The uncertainty of TMY generation has been discussed in reference [7, 8]. The number of days (N) in each month of the year when the water temperature in the storage tank reaches or exceeds the specified demand temperature was determined by hour-by-hour simulation carried out using TRNSYS [8]. SWH simulations were carried out for the 147 European sites listed in Table 3.

Table 2 System parameters for the base case

Parameter	Value
Solar collector area (A_{sc})	2 m ²
Daily hot water consumption (V_{day})	100 l day ⁻²
Storage tank volume (V_{st})	100 l
Mass flowrate	50 l m ⁻² h ⁻¹
Collector slope angle (θ)	Local latitude
Collector thermal losses coefficient ($F_R U_L$)	7 W m ⁻² K ⁻¹
Collector optical efficiency $F(\tau\alpha)$	0.8
Initial temperature (t_0) ^a	10 °C
Mode of hot water consumption	Nighttime consumption
Storage tank	Well-mixed, well-insulated

^aInitial daily water temperature in storage tank for all days of the year.

Table 3 Total solar radiation on a horizontal surface for different times of the year and for different locations in Europe

Location	Latitude (°N)	Longitude (°E)	Altitude (m)	Total annual solar radiation on horizontal surface (kW h m ⁻²)	Total solar radiation on horizontal surface from April to September (kW h m ⁻²)	Total solar radiation on horizontal surface from June to August (kW h m ⁻²)
Aberporth (UK)	52	-5	1	1045	814	450
Alghero (Italy)	41	8	0	1628	1155	647
Almeria (Spain)	37	-2	0	1738	1144	614
Amendola (Italy)	42	16	91	1540	1083	596
Ancona (Italy)	44	14	1	1383	1020	570
Athinai (Athens, Greece)	38	24	154	1582	1109	610
Badajoz/Talavera (Spain)	39	-7	168	1604	1125	633
Banja Luka (Bosnia Hercegovina)	45	17	162	1277	937	522
Barcelona (Spain)	41	2	1	1371	927	511
Bari (Italy)	41	17	0	1586	1124	610
Beograd (Serbia)	45	20	59	1395	1003	553
Bergen (Norway)	60	5	7	829	682	380
Bitola (Macedonia)	41	21	583	1603	1125	626
Bologna (Italy)	45	11	102	1289	943	528
Bolzano (Italy)	46	11	1002	1231	885	483
Boulogne Sur Seine (France)	51	2	30	1203	911	495
Braganca (Portugal)	42	-7	582	1730	1247	708
Bratislava (Slovakia)	48	17	132	1190	918	505
Bremen (Germany)	53	9	3	945	741	403
Brest (France)	48	-4	76	1139	842	467
Brindisi (Italy)	41	18	16	1602	1136	637
Brussels-Uccle (Belgium)	51	4	77	971	754	419
Bucuresti (Romania)	45	26	71	1421	1041	577
Budapest (Hungary)	47	19	103	1209	914	512
Burgos (Spain)	42	-4	861	1381	989	555
Cagliari/Elmas (Italy)	39	9	22	1591	1101	618
Ciudad Real (Spain)	39	-4	630	1616	1111	615
Cluj/Napoca (Romania)	47	24	354	1307	960	537
Coimbra (Portugal)	40	-8	46	1619	1090	597
Constanta (Romania)	44	29	1	1427	1050	588
Copenhagen (Denmark)	56	13	1	1031	842	483
Craiova (Romania)	44	24	108	1383	997	565
Crotone (Italy)	39	17	1	1639	1137	625
De Bilt (Netherlands)	52	5	3	991	774	434
Debrecen (Hungary)	47	22	122	1194	897	499
Den Helder/De Koog (Netherlands)	53	5	1	1086	856	479
Dijon (France)	47	5	236	1309	973	546
Eskdalemuir (UK)	55	-3	237	835	659	372
Evora (Portugal)	39	-8	202	1840	1292	723
Faro (Portugal)	37	-8	1	1805	1238	677
Florence (Italy)	44	11	91	1304	995	568
Funchal (Madeira)	33	-17	0	1739	1101	573
Galati (Romania)	46	28	2	1441	1046	582
Gdansk (Poland)	54	19	15	1076	857	483
Geisenheim (Germany)	50	8	84	1037	808	448
Gela (Italy)	37	14	0	1784	1202	653
Genova/Sestri (Italy)	44	9	68	1151	829	464
Graz University (Austria)	47	15	355	1127	820	451
Groningen/Eelde (Netherlands)	53	7	3	1015	801	454
Hamburg-Sasel/Fuhlsbuttelt (Germany)	54	10	31	978	783	447
Helsinki/Ilmala (Finland)	60	25	26	994	850	509
Hohenpeissenberg (Germany)	48	11	798	1213	856	465
Iasi (Romania)	47	28	77	1323	982	550
Jokioinen (Finland)	61	24	114	947	809	480
Karlstad (Sweden)	59	13	41	1048	880	521
Kassel (Germany)	51	9	155	981	764	419
Kaunas (Lithuania)	55	24	94	890	707	407
Kiev (Ukraine)	50	31	169	1060	825	483
Klagenfurt-Flughafen (Austria)	47	14	431	1254	915	500
Kolobrzeg (Poland)	54	16	49	1091	892	517
Kopaonik (Serbia)	43	21	1394	1349	907	517
La Coruna (Spain)	43	-8	0	1166	768	416
Lerwick (UK)	60	-1	0	788	659	377
Lille (France)	51	3	25	1088	818	453

Continued

Table 3 Continued

Location	Latitude (°N)	Longitude (°E)	Altitude (m)	Total annual solar radiation on horizontal surface (kW h m ⁻²)	Total solar radiation on horizontal surface from April to September (kW h m ⁻²)	Total solar radiation on horizontal surface from June to August (kW h m ⁻²)
Limoges (France)	46	1	298	1261	921	512
Lisboa (Portugal)	39	-9	16	1727	1193	665
Ljubljana/Bezigrad (Slovenia)	46	15	300	1091	829	462
Lomnický štít (Slovakia)	49	20	2073	1315	873	427
London (UK)	52	0	15	897	698	398
Lyon/Bron (France)	46	5	200	1252	945	533
Maastricht/Beek (Netherlands)	51	6	117	1006	779	431
Madrid (Spain)	40	-4	589	1593	1124	626
Malaga (Spain)	37	-4	0	1706	1144	632
Messina (Italy)	38	16	1	1616	1111	614
Milano/Linate (Italy)	45	9	99	1241	935	526
Milesovka (Czech Republic)	51	14	450	1165	882	477
Minsk (Belarus)	54	28	199	948	756	435
Moscow (Russia)	56	38	150	959	774	466
Murcia (Spain)	38	-1	25	1804	1188	654
Nancy/Essey (France)	49	6	235	1130	865	484
Nantes (France)	47	-2	5	1223	905	506
Napoli/Capodichino (Italy)	41	14	75	1529	1075	602
Negotin (Serbia)	44	23	85	1506	1102	613
Nice (France)	44	7	0	1551	1096	608
Nîmes-Courbessac (France)	44	4	75	1553	1113	637
Norderney (Germany)	54	7	2	1021	813	444
Nuernberg (Germany)	50	11	308	1052	804	443
Odessa (Ukraine)	46	31	41	1280	980	555
Olbia/Costa Smeralda (Italy)	41	10	0	1544	1098	615
Oslo-Blindern (Norway)	60	11	60	880	721	398
Ostrava/Poruba (Czech Republic)	50	18	253	1022	781	434
Pantelleria Island (Italy)	37	12	830	1687	1149	640
Pecs/Pogány (Hungary)	46	18	165	1338	995	533
Perpignan (France)	43	3	48	1532	1060	591
Pescara (Italy)	42	14	7	1445	1028	563
Pisa/S.Giusto (Italy)	44	10	3	1400	1001	553
Pleven (Bulgaria)	43	25	114	1259	903	494
Porto Santo (Madeira)	33	-16	176	1723	1122	597
Porto/Serra Do Pilar (Portugal)	41	-9	91	1643	1149	637
Praha/Karlovy Vary (Czech Republic)	50	14	245	997	772	431
Pristina (Serbia)	43	21	653	1418	1004	558
Qrendi (Malta)	36	14	48	1897	1269	700
Reims (France)	49	4	99	1139	856	471
Reykjavik (Iceland)	64	-22	16	779	674	381
Riga (Latvia)	57	24	5	898	749	433
Roma/Ciampino (Italy)	42	13	141	1529	1079	601
Rouen (France)	49	1	10	1106	838	464
Saarbrücken (Germany)	49	7	200	1052	812	458
Salzburg-Flughafen (Austria)	48	13	453	1068	777	423
Sandanski (Bulgaria)	42	23	297	1406	997	565
Sarajevo (Bosnia Hercegovina)	44	18	524	1260	903	504
Schleswig (Germany)	55	10	15	959	774	433
Sevilla/San Pablo (Spain)	37	-6	16	1190	720	364
Sofia Observatory (Bulgaria)	43	23	592	1157	830	467
Sonnblick (Austria)	47	13	2429	1391	944	481
Split/Marjan (Croatia)	44	16	62	1637	1151	640
St Petersburg/Voikovo (Russia)	60	30	5	746	646	379
St Hubert (Belgium)	50	5	480	1029	793	441
Stockholm (Sweden)	60	18	16	1032	866	511
Stuttgart (Germany)	49	9	415	1140	855	470
Suwalki (Poland)	54	23	171	1060	852	497
Szeged (Hungary)	46	20	76	1274	946	520
Tbilisi (Georgia)	41	45	405	1335	961	536
Timisoara (Romania)	46	21	91	1330	981	547
Toulon (France)	43	6	0	1670	1186	674
Toulouse Blagnac (France)	44	1	130	1384	981	542
Trapani/Birgi (Italy)	38	13	1	2007	1336	760
Trier-Petrisberg (Germany)	50	7	158	1065	825	458

Continued

Table 3 Continued

Location	Latitude (°N)	Longitude (°E)	Altitude (m)	Total annual solar radiation on horizontal surface (kW h m ⁻²)	Total solar radiation on horizontal surface from April to September (kW h m ⁻²)	Total solar radiation on horizontal surface from June to August (kW h m ⁻²)
Trieste (Italy)	46	14	109	1236	898	500
Trikala (Greece)	41	23	4	1112	792	441
Tromso-Langnes (Norway)	70	19	27	652	592	369
Trondheim (Norway)	63	10	100	843	719	414
Ustica Is. (Italy)	39	13	0	1718	1168	642
Valencia (Spain)	39	0	8	1549	1040	573
Valentia (Ireland)	52	-10	10	1039	804	437
Valladolid (Spain)	42	-5	704	1495	1070	603
Varna (Bulgaria)	43	28	80	1256	900	505
Venezia/Tessera (Italy)	46	12	2	1289	951	538
Visby (Sweden)	58	18	50	1102	914	537
Vlissingen (Netherlands)	51	4	1	1050	814	454
Warsaw-Okęcie (Poland)	52	21	94	966	787	459
Wien/Hohe Warte (Austria)	48	16	600	1105	844	469
Wuerzburg (Germany)	50	10	209	1115	854	471
Zagreb/Gric (Croatia)	46	16	400	1211	909	503
Zaragoza (Spain)	42	-1	207	1588	1112	619
Zlatibor (Bosnia Hercegovina)	44	20	794	1342	931	513
Zuerich/Kloten (Switzerland)	47	9	480	1134	866	485

3 RESULTS

The number of days that the temperature of water in the storage tank reaches or exceeds specified demand temperatures as a function of total solar radiation and collector surface area for different time periods is shown in Figs 2 to 4 for the whole year, Figs 5 to 7 for the warm half-year period (i.e. April to September), and Figs 8 to 10 for summer (i.e. June to August). Each figure shows results for demand temperatures of 37, 45, and 55 °C. In

continental Europe, monthly average solar heated water temperatures are broadly lower for higher latitudes. Figs 2 to 10 show that there is a clear dependence of the 'number of days' on total solar radiation for all three time-periods considered (i.e. whole year, warm half-year, and summer) and at all three demand temperatures considered (i.e. 37, 45, and 55 °C). Significant deviation from general trends may be seen for results corresponding to Lomnický Stit (Slovakia), Sonnblick (Austria), and Kopaonik (Serbia). These high altitude locations

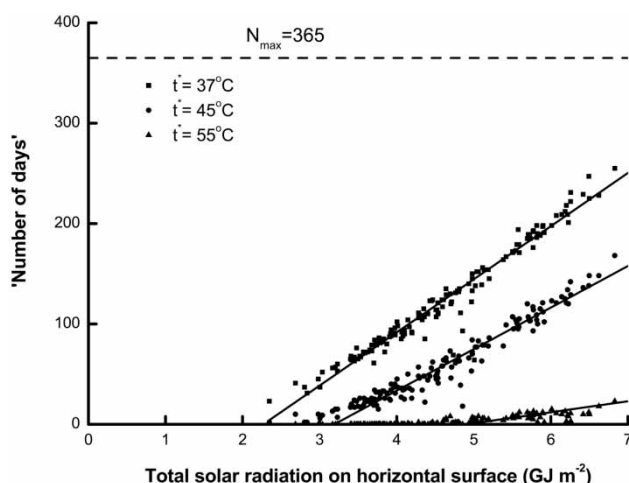


Fig. 2 The number of days for which the temperature of water in the storage tank reaches or exceeds specified demand temperatures as a function of daily total solar radiation on horizontal surface for a collector area of 1 m² and for the whole year

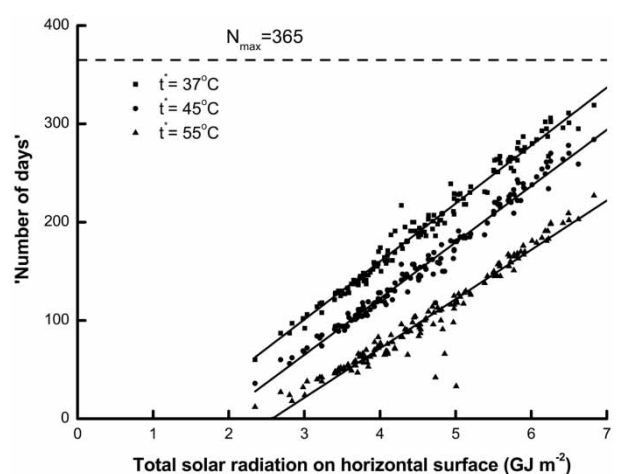


Fig. 3 The number of days for which the temperature of water in the storage tank reaches or exceeds specified demand temperatures as a function of daily total solar radiation on horizontal surface for a collector area of 2 m² and for the whole year

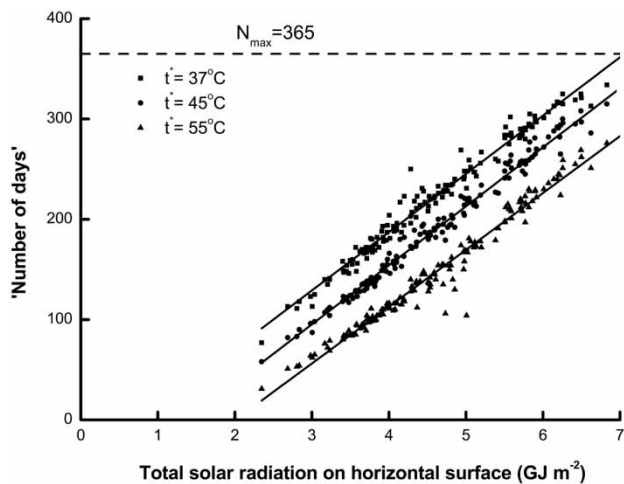


Fig. 4 The number of days for which the temperature of water in the storage tank reaches or exceeds specified demand temperatures as a function of daily total solar radiation on horizontal surface for a collector area of 3 m² and for the whole year

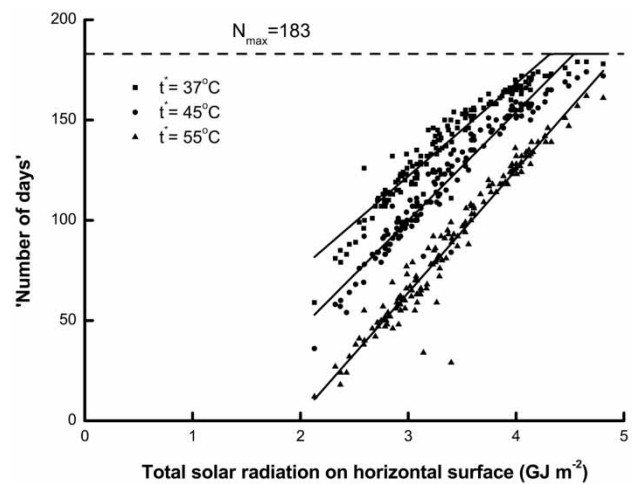


Fig. 6 The number of days for which the temperature of water in the storage tank reaches or exceeds specified demand temperatures as a function of daily total solar radiation on horizontal surface for a collector area of 2 m² and for the period April to September

combine high solar radiation with relatively low-ambient temperatures. For these locations, the relative dispersion of data increases with increasing total solar radiation. This is because in mountainous areas, there are wide differences in ambient temperature (the principal determinant of heat loss from the collector) for similar levels of insolation. Contour maps of the variation of ‘number of days’ are shown in Figs 11 to 13 for demand temperatures of 37, 45, and 55 °C, respectively.

4 CORRELATION OF TYPICAL SWH PERFORMANCE

For a specified demand temperature, the number of days that specified hot water demand temperature could be satisfied, N , may be assumed to depend solely on the total insolation for the period of year considered. For a particular demand temperature, demand profile and system specification, N , may then be determined for any location solely as a

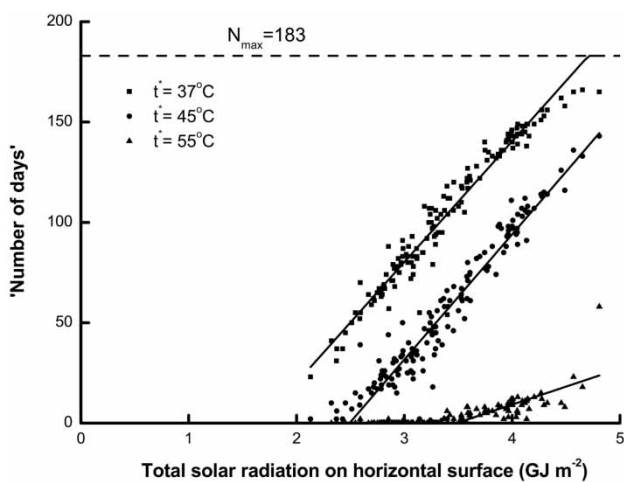


Fig. 5 The number of days for which the temperature of water in the storage tank reaches or exceeds specified demand temperatures as a function of daily total solar radiation on horizontal surface for a collector area of 1 m² and for the period April to September

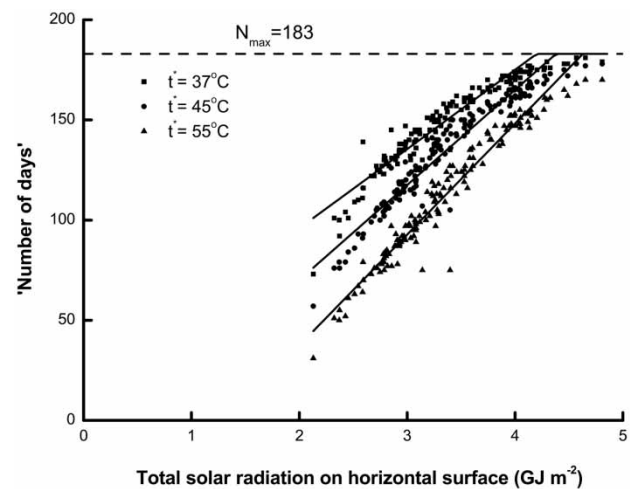


Fig. 7 The number of days for which the temperature of water in the storage tank reaches or exceeds specified demand temperatures as a function of daily total solar radiation on horizontal surface for a collector area of 3 m² and for the period April to September

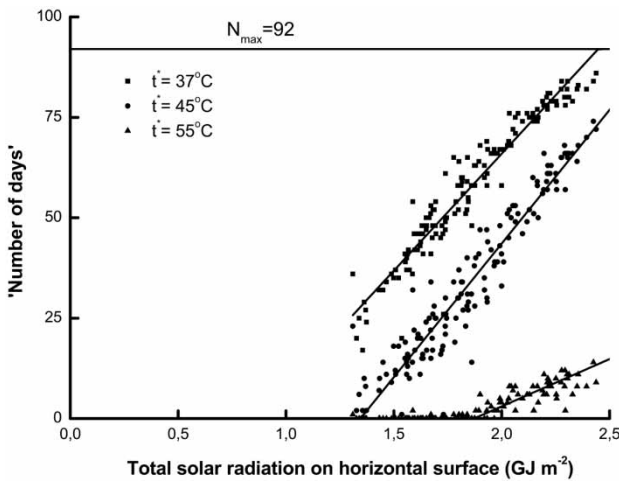


Fig. 8 The number of days for which the temperature of water in the storage tank reaches or exceeds specified demand temperatures as a function of daily total solar radiation on horizontal surface for a collector area of 1 m² and for the period June to August

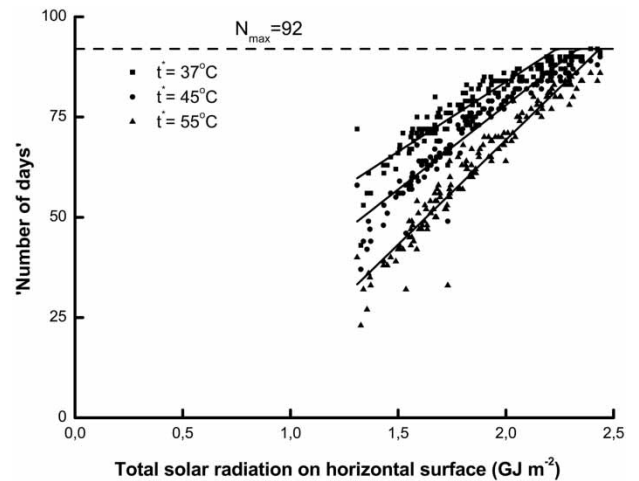


Fig. 10 The number of days for which the temperature of water in the storage tank reaches or exceeds specified demand temperatures as a function of daily total solar radiation on horizontal surface for a collector area of 3 m² and for the period June to August

function of total insolation. A correlation between number of days and total solar radiation has the form

$$N = \begin{cases} 0 & \text{for } I < I_0 \\ \frac{(I - I_0)}{(I_{\max} - I_0)} N_{\max} & \text{for } I_0 \leq I \leq I_{\max} \\ N_{\max} & \text{for } I > I_{\max} \end{cases} \quad (1)$$

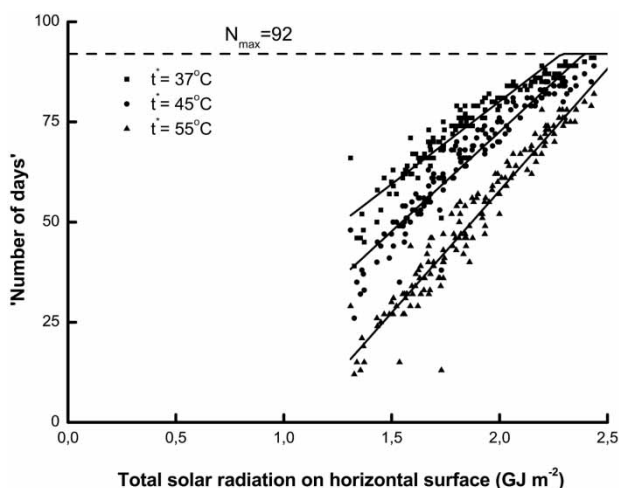


Fig. 9 The number of days for which the temperature of water in the storage tank reaches or exceeds specified demand temperatures as a function of daily total solar radiation on horizontal surface for a collector area of 2 m² and for the period June to August

For summer, $N_{\max} = 92$ days; for April to September, $N_{\max} = 183$ days; and for the whole year, $N_{\max} = 365$ days. If the total solar radiation is less than a minimum threshold value of total solar radiation on horizontal surface, I_0 , then the SWH will be unable to heat water to the specific demand temperature. The minimum threshold insolation increases with increase in specific demand temperature and decreases with increasing solar collector area per unit store volume. The number of days during which the solar heated water temperature exceeds the specified demand temperature is limited to the total number of days in the period under consideration. When the total number of days is reached, the water temperature in SWH storage tank will obviously exceed the specific demand temperature for every day within the period. The latter is associated with a maximum threshold value of insolation, I_{\max} . I_0 and I_{\max} depend on the solar collector area and the duration of the period under consideration with relationships of the form

$$I_0 = a \cdot \exp\left(\frac{b}{A_{sc}}\right) \quad (2a)$$

$$I_{\max} = c \cdot \exp\left(\frac{d}{A_{sc}}\right) \quad (2b)$$

Coefficients ‘a’, ‘b’, ‘c’, and ‘d’ have been obtained from calculations using the least-squares method; the values of these coefficients are given in Table 4 are only valid for collector areas in the

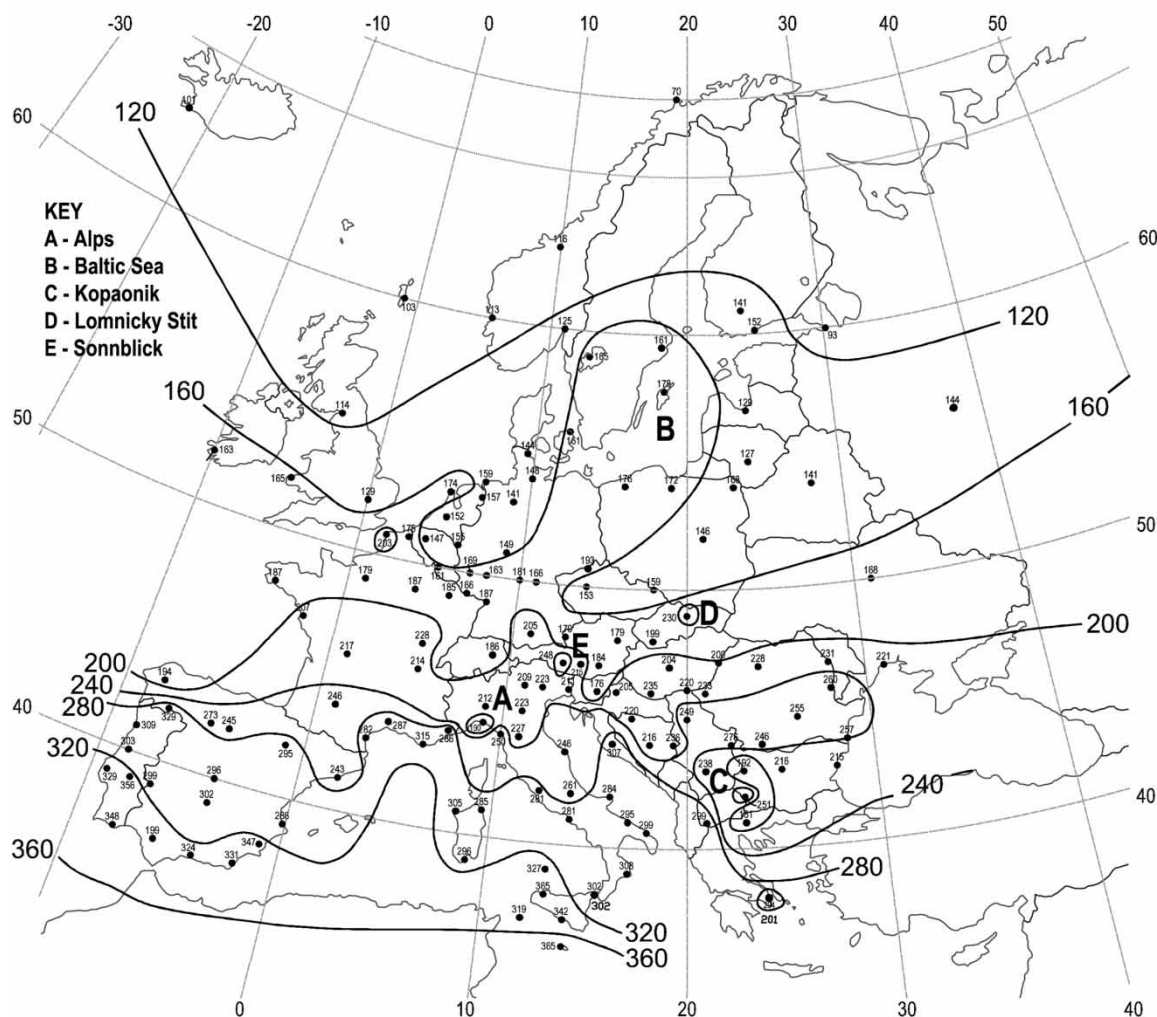


Fig. 11 Contour maps of the number of days in a year for which the temperature of water in the storage tank reaches or exceeds 37 °C for Europe

range 1–4 m² and total solar radiation on horizontal surface in the range 1.08–2.16 GJ m² for summer, 1.8–3.6 GJ m^{−2} for the warm half-year, and 2.52–5.4 GJ m^{−2} when the whole year is considered. The inaccuracy in determining the number of days for which a specified demand temperature is satisfied arising from using equations (1) and (2) is in the range 10–30 per cent due to the approximation error; the error is the smallest for high values of total solar radiation.

5 SENSITIVITY OF SWH PERFORMANCE TO SOLAR COLLECTOR PARAMETERS

Many solar collectors have one transparent cover and do not have a selective coating [10, 11]. Their overall heat loss coefficient (U_L) varies in the range 5.5–7.0 W m^{−2} K^{−1} and their optical coefficient ($\tau\alpha$)

varies in the range 0.78–0.8. As the range of $\tau\alpha$ is small, sensitivity analysis has been carried out only for U_L . As A_{sc} increases, N depends more on insolation and the influence of U_L on N is reduced. Data dispersion depends mainly on geographical location of sites; the other parameters are the periods of year, specific demand temperature, and A_{sc} considered. Considering this dispersion as random, the influence of U_L can be estimated [12] for the European locations considered

$$\left\langle \frac{N_{U_L = 5}}{N_{U_L = 7}} \right\rangle = 1.13 \pm 0.008;$$

$$\left\langle \frac{N_{U_L = 9}}{N_{U_L = 7}} \right\rangle = 0.86 \pm 0.008$$

(3)

where brackets denote averaging for all variants. Thus, U_L changing from 7 to 5 W m^{−2} K^{−1} increases

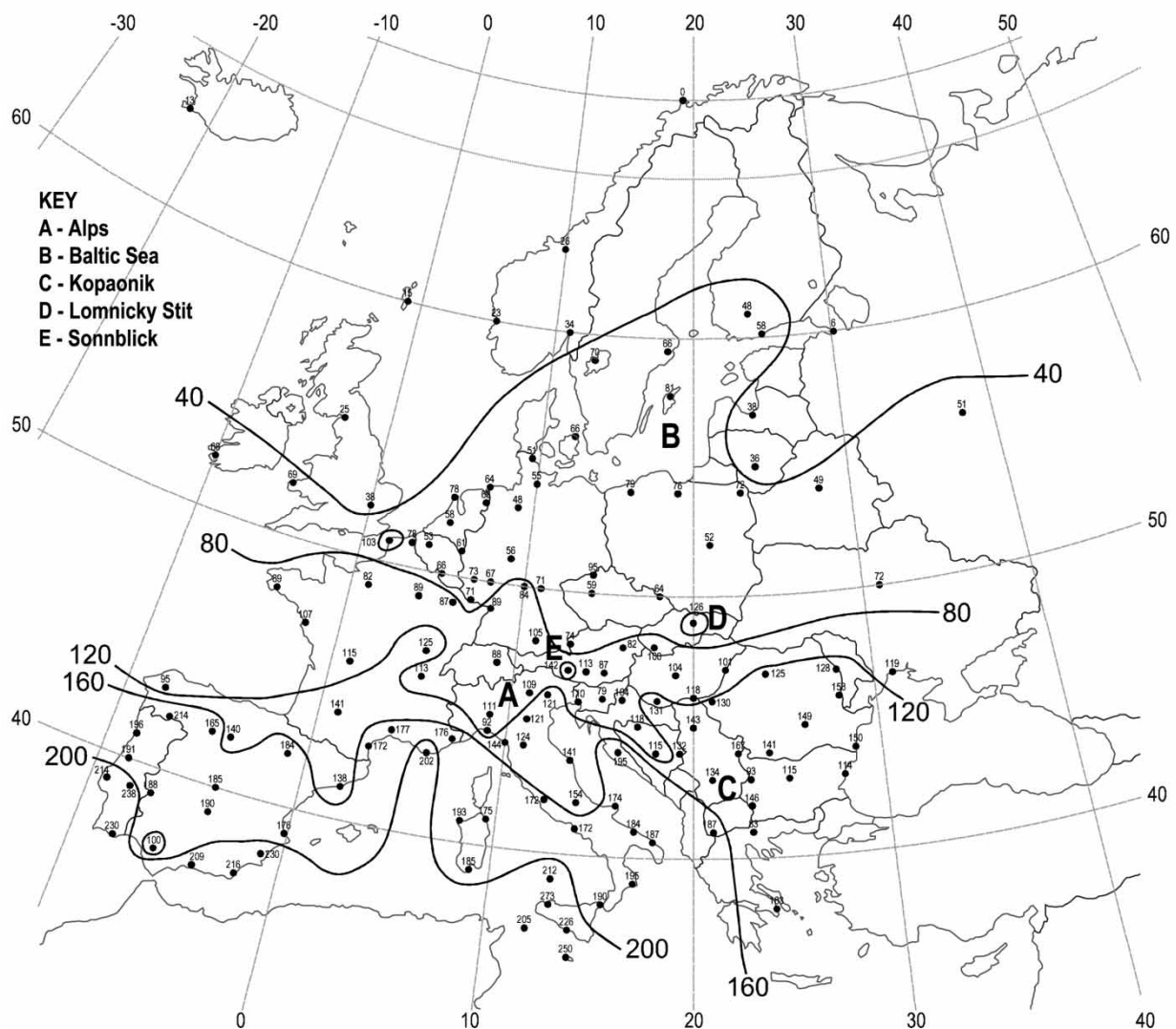


Fig. 12 Contour maps of the number of days in a year for which the temperature of water in the storage tank reaches or exceeds 45 °C for Europe

N by 13 per cent and increasing of U_L from 7 to 9 W m⁻² K⁻¹ decreases this value by 14 per cent.

6 CORRELATION BETWEEN 'NUMBER OF DAYS' AND 'SOLAR A FRACTION'

The results of calculation of 'number of days' and 'solar fractions' for SWH with storage tank volume of 100 l and daily water consumption of 100 l day⁻¹ for two periods of SWH operation (whole year and April to September) and all considered sites in Europe are shown in Fig. 14. For both cases, the solar collector surface area was varied in range of 1–4 m²; the specified demand temperatures were 37, 45, and 55 °C. The solar fraction for each day is calculated as shown below, where the initial

temperature of the water in the storage tank is 10 °C.

$$f = 1 - \frac{Q_{\text{aux}}}{Q_{\text{tot}}} \quad (4)$$

If solar preheated water temperature to the end of a day was equal to or higher than the demand temperature, the solar fraction was considered as equal to 1. Average solar fraction for both considered periods of year was calculated as the ratio of the sum of daily solar fractions to the amount of days in the period. N was normalized to the amount of days in each period too.

All correlation data points were plotted on a graph of normalized 'number of days' versus average solar fraction for considered periods of year as shown in Fig. 14. The lower the normalized number of days,

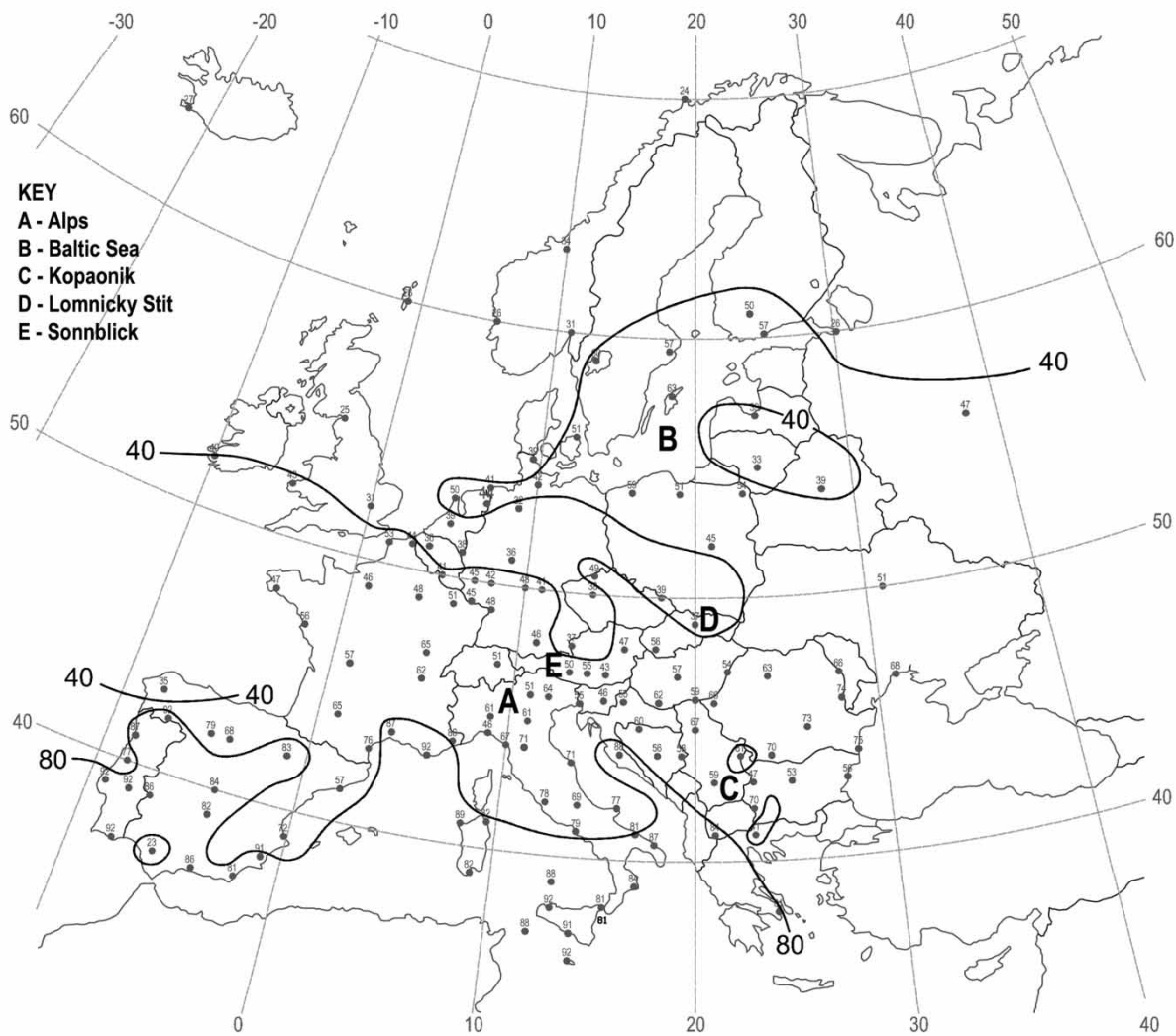


Fig. 13 Contour maps of the number of days in a year for which the temperature of water in the storage tank reaches or exceeds 55 °C for Europe

the wider data arrays distribution along the solar fraction axis. For higher values of solar fractions and specific number of days, there was less spread of data points.

7 CONCLUSION

Correlations have been established for the number of days a specified hot water demand temperature can

Table 4 Coefficients for the determination of the maximum and minimum threshold total solar radiation on horizontal surface as functions of demand temperature and period of year

Period of year	Demand temperature (°C)	Coefficients for I_0				Coefficients for I_{max}			
		a (GJ m ⁻²)	Δ (%)	b (GJ m ⁻²)	Δ (%)	c (GJ m ⁻²)	Δ (%)	d (GJ m ⁻²)	Δ (%)
Whole year	37	0.86	4.17	0.93	6.45	5.8	0.68	0.57	1.75
	45	1.09	2.3	1.01	2.97	5.36	3.42	1.08	3.7
	55	1.3	1.93	1.23	4.07	5.79	0.37	1.38	0.72
April to September	37	0.54	26.67	1.4	21.43	3.6	1	0.23	8.7
	45	0.97	8.15	1.01	9.9	3.53	1.33	0.43	8.7
	55	1.22	3.82	1.18	8.47	3.53	0.92	0.63	3.17
June to August	37	0.35	18.75	1.2	16.67	1.9	0.38	0.18	5.56
	45	0.54	6	1.01	7.92	1.92	1.12	0.32	6.25
	55	0.65	7.78	1.2	16.67	1.94	1.48	0.5	8

Δ (%) is the maximum error in each case.

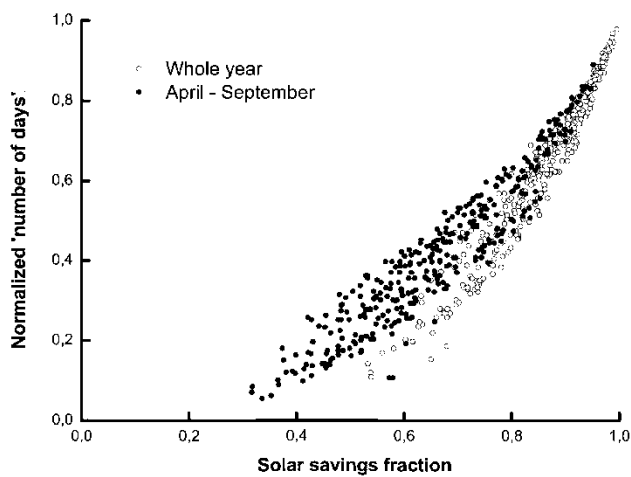


Fig. 14 A comparison of the number of days for which the temperature of water in the storage tank reaches or exceeds specified demand temperatures and solar fractions for Europe for the whole year and for the period April to September

be satisfied by a SWH without the use of auxiliary heating for 147 European locations for a whole and part year periods. The accuracy in determining the number of days is in the range 10–30 per cent; the error is the smallest for higher values of total insolation. An example of using the correlation to estimate the performance of a SWH for any location in Europe is provided in Appendix 2 for solar collectors with areas and specifications corresponding to those used in this study. If the latter is not the case, the 'number of days' and the terms I_0 and I_{\max} may be calculated using equations (1) and (2), respectively. The coefficients a , b , c , and d may be obtained from Table 4 for the period under consideration.

Figures 11 to 13 show that with increasing altitude, particularly in the Alps, contours deviate with greater irregularity from a broad alignment with latitude. The effect of higher summer ambient temperatures associated with the prevailing continental climate in northern Europe can also be seen in the form of the contours in the region of the southern Baltic Sea.

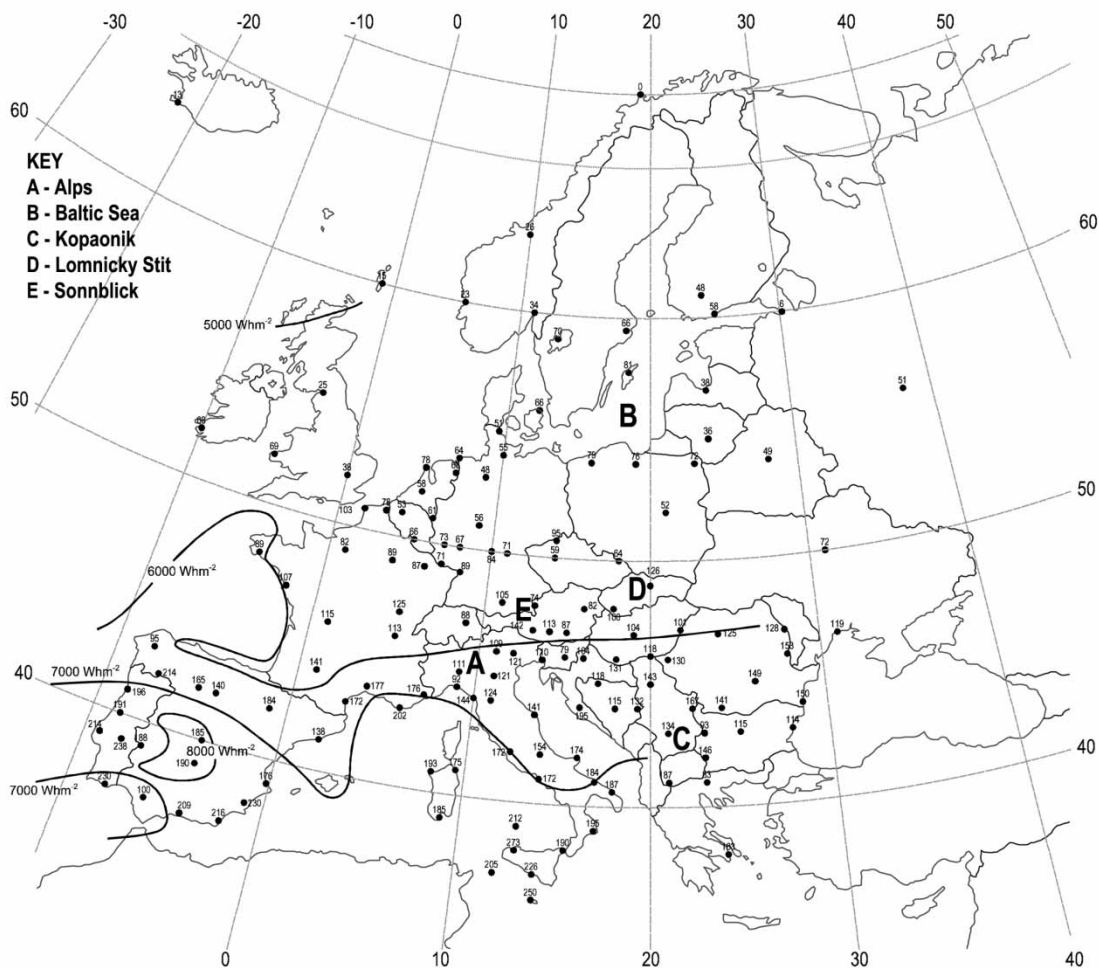


Fig. 15 Mean monthly cumulative daily global insolation on a horizontal plane for July (based on 1985 to 2000 Meteosat data)

(As solar energy collection is more limited in winter, the cold winters also associated with a continental climate have less effect.) Higher demand temperatures entail a larger difference between SWH and ambient temperatures and thus increased system heat loss. As they influence ambient temperature, both altitude and continental climate effects on heat loss become more pronounced at higher demand temperatures. In south-west Spain, maritime cloud cover leads to lower insolation in south-west Spain as shown in Fig. 15 in the crucial summer period.

In colder part of year, there are more days when water is not heated to the specified demand temperatures, therefore in Fig. 14, whole year date points sit below April-to-September data. The solar fraction threshold below which the normalized number of days is zero is 0.3 for April to September and 0.5 for the whole year. (These values for the whole of Europe are very similar to those for London and Northern Ireland [5] conditions.) It is thus not possible for the particular SWH considered to provide hot water at a specified demand temperature of 37 °C or above throughout the year without the use of auxiliary heating at any location in Europe.

Taken with cost and product quality information, the production of contour maps as described in this paper to show the geographic variation of the performance of different SWH would aid both system selection for designers and the definition of appropriate markets for manufacturers.

REFERENCES

- Morrison, G. L.** *Solar water heating in solar energy: the state of the art* (Ed. J. Gordon) 2001 (James and James Publishers Ltd, London, UK).
- Urbschat, C.** *Sunrise 2002: die europaischen markte fur solarthermie und photovoltaik*, 2002 (Eclareon GmbH, Berlin, Germany).
- Reddy, T. A.** *The design and sizing of active solar thermal systems*, 1987 (Clarendon Press, Oxford, UK).
- Bourges, B.** *European simplified methods for active solar system design*, 1991 (Kluwer Academic Publishers, Dordrecht, The Netherlands).
- Yohanis, Y. G., Popel, O., Frid, S. E., and Norton, B.** Analysis of the annual number of days for which solar heated water can be provided above a specified demand temperature. *Sol. Energy*, 2005, in press.
- Beckman, W. A., Klein, S. A., and Duffie, J. A.** *Solar heating design by the f-chart method*, 1977 (Wiley-Interscience, New York).
- Duffie, J. A. and Beckman, W. A.** *Solar engineering of thermal processes*, 1980 (Wiley, New York).
- Klein, S. A., Duffie, J. A., Mitchell, J. C., Kummer, J. P., Beckmann, W. A., Duffie, N. A., Braun, J. E., Urban, R. E., Thornton, J. W., Mitchell, J. W., Freeman, T. L., Evans, B. L., and Fiksel, A.** TRNSYS 15, a transient system simulation program. *User's manual (version*

15), 2000 (Solar Energy Laboratory, University of Wisconsin-Madison).

- Anonymous. *RETScreen international (RETScreen)*, 2000 (CANMET Energy Diversification Research Laboratory (CEDRL), Canada), available from <http://retscreen.gc.ca>.
- Weiss, W.** Come in from the cold? The solar thermal market in Europe. *Renew. Energy World*, 2002 5(4), 91–97.
- Weiss, W. and Faninger, G.** *Solar thermal collector market in IEA member countries*. Report of IEA Solar Heating and Cooling Programme, 2002.
- Zaidel, A. N.** Errors in measurement of physical values, 1974 (Science Publishers, Leningrad, Russia) (in Russian).

APPENDIX 1

Notation

$a, b, c,$ and d	coefficient
A_{sc}	solar collector surface area (m ²)
f	solar fraction
F'	solar collector flow factor
F_R	solar collector heat removal factor
I	total solar radiation on horizontal surface (GJ m ⁻²)
I_{max}	maximum threshold total solar radiation on horizontal surface (GJ m ⁻²)
I_0	minimum threshold total solar radiation on horizontal surface (GJ m ⁻²)
N	number of days a specified hot water demand temperature is met solely by solar energy
N_{max}	maximum threshold number of days a specified hot water demand temperature is met solely by solar energy
N_{U_L}	for a particular overall heat loss coefficient, the number of days a specified hot water demand temperature is met solely by solar energy
Q_{aux}	auxiliary heating requirement (J)
Q_T	useful heat produced by solar energy during the lifetime of SWH (J)
Q_{tot}	total energy required to heat the supply water to the demand temperature (J)
t^*	specified demand water temperature in storage tank (°C)
U_L	overall heat loss coefficient (W m ⁻² K ⁻¹)
V_{day}	daily hot water requirement (l day ⁻¹)
V_{st}	storage volume (l)
$\tau\alpha$	optical coefficient

APPENDIX 2

As an example of the estimation of the performance of SWH using the correlation developed earlier, a SWH at Kew near London is considered. The total insolation on a horizontal surface for whole year, half-year, and summer are 3.23, 2.51, and 1.43 GJ m^{-2} , respectively [9].

To estimate the solar collector area (A_{sc}) for a half-year operating period, the following procedure is adopted. For a daily hot water requirement $V_{\text{day}} = 100$ l, using Fig. 5, determine the 'number of days' (N) for a specified temperature (t^*) for 2.51 GJ m^{-2} total insolation on a horizontal surface for half-year period operation for collector areas (A_{sc}) of 1, 2, and 3 m^2 :

- (a) for $A_{\text{sc}} = 1 \text{ m}^2$ and $t^* \geq 37^\circ\text{C}$, $N = 50$ days;
- (b) for $A_{\text{sc}} = 1 \text{ m}^2$ and $t^* \geq 45^\circ\text{C}$, $N = 5$ days;
- (c) for $A_{\text{sc}} = 1 \text{ m}^2$ and $t^* \geq 55^\circ\text{C}$, $N = 0$ days.

If the 'number of days' obtained using a collector area of 1 m^2 does not meet the requirement, then

Fig. 6 is used to determine N for a collector area of 2 m^2 . As earlier, N is determined as follows:

- (a) for $A_{\text{sc}} = 2 \text{ m}^2$ and $t^* \geq 37^\circ\text{C}$, $N = 100$ days;
- (b) for $A_{\text{sc}} = 2 \text{ m}^2$ and $t^* \geq 45^\circ\text{C}$, $N = 70$ days;
- (c) for $A_{\text{sc}} = 2 \text{ m}^2$ and $t^* \geq 55^\circ\text{C}$, $N = 35$ days.

This procedure is repeated for a collector area of 3 m^2 as shown subsequently:

- (a) for $A_{\text{sc}} = 3 \text{ m}^2$ and $t^* \geq 37^\circ\text{C}$, $N = 130$ days;
- (b) for $A_{\text{sc}} = 3 \text{ m}^2$ and $t^* \geq 45^\circ\text{C}$, $N = 85$ days;
- (c) for $A_{\text{sc}} = 3 \text{ m}^2$ and $t^* \geq 55^\circ\text{C}$, $N = 65$ days.

This is based on daily consumption of 100 l and a storage volume of 100 l as well. If the required daily consumption is different, say 300 l, a scaling method can be applied. The storage volume as earlier will be taken to be the same as the daily requirement, i.e. 300 l. The collector area (A_{sc}) is scaled by the ratio of daily requirement to storage, i.e. $A_{\text{sc}} (V_{\text{day}}/V_{\text{st}})$. In this case, the scaling factor will be equal to 3; this means that the new collector area will be three times larger. All the earlier calculations are based on the base case as given in Table 2.